BJP BRITISH JOURNAL OF PHARMACOLOGY

BPS BRITISH PHARMACOLOGICAL SOCIETY

BJP British Journal of Pharmacology

DOI:10.1111/j.1476-5381.2010.00987.x
www.brjpharmacol.org

RESEARCH PAPER

Pharmacogenetics of the mycophenolic acid targets inosine monophosphate dehydrogenases IMPDH1 and IMPDH2: gene sequence variation and functional genomics

T-Y Wu[1], Y Peng[2], LL Pelleymounter[1], I Moon[1], BW Eckloff[3], ED Wieben[3], VC Yee[2] and RM Weinshilboum[1]

[1]*Division of Clinical Pharmacology, Department of Pharmacology and Experimental Therapeutics, Mayo Clinic, Rochester, MN, USA,* [2]*Department of Biochemistry, Case Western Reserve University, Cleveland, OH, USA, and* [3]*Department of Biochemistry and Molecular Biology, Mayo Clinic, Rochester, MN, USA*

Correspondence
Richard M. Weinshilboum, Department of Molecular Pharmacology and Experimental Therapeutics, Mayo Clinic, 200 First Street SW, Rochester, MN 55905, USA. E-mail: weinshilboum.richard@mayo.edu

Keywords
mycophenolic acid; mycophenolate mofetil; mycophenolate sodium; inosine monophosphate dehydrogenase; *IMPDH1*; *IMPDH2*; pharmacogenetics; functional genomics; transplantation

Received
28 April 2010
Revised
22 June 2010
Accepted
14 July 2010

BACKGROUND AND PURPOSE
Inosine monophosphate dehydrogenases, encoded by *IMPDH1* and *IMPDH2*, are targets for the important immunosuppressive drug, mycophenolic acid (MPA). Variation in MPA response may result, in part, from genetic variation in *IMPDH1* and *IMPDH2*.

EXPERIMENTAL APPROACH
We resequenced *IMPDH1* and *IMPDH2* using DNA from 288 individuals from three ethnic groups and performed functional genomic studies of the sequence variants observed.

KEY RESULTS
We identified 73 single nucleotide polymorphisms (SNPs) in *IMPDH1*, 59 novel, and 25 SNPs, 24 novel, in *IMPDH2*. One novel IMPDH1 allozyme (Leu275) had 10.2% of the wild-type activity as a result of accelerated protein degradation. Decreased activity of the previously reported IMPDH2 Phe263 allozyme was primarily due to decreased protein quantity, also with accelerated degradation. These observations with regard to the functional implications of variant allozymes were supported by the IMPDH1 and IMPDH2 X-ray crystal structures. A novel *IMPDH2* intron 1 SNP, G > C IVS1(93), was associated with decreased mRNA quantity, possibly because of altered transcription.

CONCLUSIONS AND IMPLICATIONS
These results provide insight into the nature and extent of sequence variation in the *IMPDH1* and *IMPDH2* genes. They also describe the influence of gene sequence variation that alters the encoded amino acids on IMPDH function and provide a foundation for future translational studies designed to correlate sequence variation in these genes with outcomes in patients treated with MPA.

Abbreviations
3MA, 3-methyladenine; AA, African-American; CA, Caucasian-American; EMS, electrophoretic mobility shift; FR, flanking region; HCA, Han Chinese-American; IMPDH, inosine monophosphate dehydrogenase; MPA, mycophenolic acid; qRT-PCR, quantitative reverse transcription polymerase chain reaction; RRL, rabbit reticulocyte lysate; SDS-PAGE, sodium dodecyl sulphate polyacrylamide gel electrophoresis; SNP, single nucleotide polymorphism; WT, wild-type

Introduction

The immunosuppressant drug mycophenolic acid (MPA) inhibits inosine monophosphate dehydrogenase (IMPDH) and is used to prevent rejection in solid organ transplantation patients (Allison and Eugui, 2000). MPA is also used to treat autoimmune diseases (Mak *et al.*, 2009) and multiple myeloma (Takebe *et al.*, 2004). IMPDH catalyses the rate-limiting step in *de novo* guanosine monophosphate synthesis. Because lymphocytes rely on *de novo* synthesis to provide guanine nucleotides while most other cells use the salvage pathway, inhibition of IMPDH results in immunosuppression (Allison and Eugui, 2000). However, in addition to having a narrow therapeutic index, clinical response to MPA is quite variable, and is complicated by large individual variation in both MPA plasma concentrations (Pisupati *et al.*, 2005; Fernandez *et al.*, 2007) and levels of IMPDH activity (Glander *et al.*, 2001; 2004).

Two different IMPDH isoforms are encoded by *IMPDH1* and *IMPDH2* (Gu *et al.*, 1997; Zimmermann *et al.*, 1997). Both isoforms are cytosolic, but they are known to be able to aggregate (Ji *et al.*, 2006). *IMPDH1* spans 18 kb on chromosome 7q31.3, encoding seven splice variants as a result of differential splicing (Gu *et al.*, 1997; Spellicy *et al.*, 2007). We focused our studies on the canonical 514 amino acid IMPDH1 isoform. *IMPDH2* is 5 kb in length and maps to chromosome 3p21.2 (Zimmermann *et al.*, 1995). Although the two isoforms have similar substrate kinetics (Carr *et al.*, 1993), the two gene products are not redundant. *IMPDH2* expression is inducible and, thus, it is more highly expressed in many tissues than the constitutively expressed *IMPDH1* (Senda and Natsumeda, 1994). Knockout of *IMPDH2* is embryonic lethal in mice (Gu *et al.*, 2000), but *IMPDH1* knockout mice are phenotypically normal (Gu *et al.*, 2003). Despite their differences, inhibition of both IMPDH1 and IMPDH2 is important for the antiproliferative effects of MPA (Wu, 1994; Allison and Eugui, 2000).

Genetic polymorphisms in both *IMPDH1* and *IMPDH2* have been shown to influence outcome in transplantation patients treated with MPA, suggesting that response to MPA might be influenced, in part, by inheritance. Examples include a nonsynonymous single nucleotide polymorphism (SNP) in *IMPDH2* that was shown to reduce IMPDH activity (Wang *et al.*, 2007), an *IMPDH2* intron SNP that increased IMPDH activity in MPA-treated transplantation patients (Sombogaard *et al.*, 2009), an *IMPDH2* intron SNP that reduced the antiproliferative effects of MPA on lymphocytes (Winnicki *et al.*, 2010), and two *IMPDH1* intron SNPs associated with biopsy-proven acute transplant rejection (Wang *et al.*, 2008). Therefore, we performed a comprehensive study of sequence variation in *IMPDH1* and *IMPDH2* by resequencing DNA from 288 unrelated individuals in three ethnic groups, followed by functional studies of the variants observed. These results shed light on possible mechanisms by which IMPDH activity might be altered by gene sequence variation and they provide a foundation for future pharmacogenetic studies of variation in MPA response in transplant patients.

Methods

DNA samples

Anonymized DNA samples from 96 African-American (AA), 96 Caucasian-American (CA) and 96 Han Chinese-American (HCA) healthy subjects (sample sets HD100AA, HD100CAU and HD100CHI) were obtained from the Coriell Institute (Camden, NJ). All subjects had provided written consent for the use of their DNA for research purposes. These studies were reviewed and approved by the Mayo Clinic Institutional Review Board.

Gene resequencing

All *IMPDH1* and *IMPDH2* exons, intron–exon splice junctions and portions of their 5′-flanking regions (FRs) were amplified using the PCR, as described previously (Moyer *et al.*, 2008). Amplification primer sequences are listed in Table S1. Amplicons were sequenced on both strands in the Mayo Molecular Biology Core Facility using dye terminator sequencing chemistry. Polymorphisms observed only once, as well as any with ambiguous chromatograms, were subjected to a second, independent round of amplification – followed by DNA sequencing.

Expression constructs

The open reading frames for *IMPDH2* and the 514 amino acid *IMPDH1* isoform were amplified from clones MGC-9332 and MGC-40351 (ATCC, Manassas, VA), respectively, and each amplicon was subcloned into pcDNA™3.1D/V5-His-TOPO (Invitrogen, Carlsbad, CA) in frame with the V5-His tag. Site-directed mutagenesis of variant allozyme constructs, transient expression and the preparation of recombinant IMPDH allozymes expressed in COS-1 cells were performed as described previously (Moyer *et al.*, 2008).

Activity assay

IMPDH activity was determined in COS-1 cell lysates using a high performance liquid chromatography assay described previously (Glander *et al.*,

2009) with IMP and NAD^+ concentrations of 1200 and 333 μM respectively. Variant allozyme activities are reported as percentages of the wild-type (WT). Co-transfection of pSV-β-galactosidase DNA made it possible to correct for variation in transfection efficiency (Moyer *et al.*, 2008). Substrate kinetic studies were performed with [IMP] ranging from 20 to 1500 μM, with [NAD^+] fixed at 333 μM and with [NAD^+] ranging from 10 to 500 μM, with [IMP] fixed at 1200 μM, using enzyme translated *in vitro* using the TNT® coupled rabbit reticulocyte lysate (RRL) system (Promega, Madison, WI).

Western blots

Levels of immunoreactive protein were determined for each allozyme by quantitative Western blot analysis performed with a rabbit polyclonal V5-tag antibody (Abcam, Cambridge, MA), as described previously (Moyer *et al.*, 2008). These results were quantified using ImageJ software (http://rsbweb.nih.gov/ij/).

RRL degradation

The RRL system was used to transcribe and translate each allozyme in the presence of [^{35}S]-methionine (PerkinElmer, Boston, MA), and the rate of protein degradation was determined as described previously (Wang *et al.*, 2003). Briefly, *in vitro* translated protein was placed in untreated RRL together with a creatine phosphate-based ATP regeneration system. This mixture was incubated at 37°C and sampled at various time points. The samples were subjected to sodium dodecyl sulphate polyacrylamide gel electrophoresis (SDS-PAGE), and the amount of allozyme protein at each time point was determined by autoradiography.

Pulse-chase assays

COS-1 cells were transiently transfected with WT or Phe263 IMPDH2. After 48 h, the transfected cells were grown in methionine-free media for 30 min, 'pulsed' with media containing 0.1 mCi·mL^{-1} [^{35}S]-methionine (PerkinElmer) for 20 min, and were then 'chased' with media containing non-radioactive methionine. Samples of the cells were taken at various time points and were processed with the Classic IP Kit (Pierce Protein Research Products, Rockford, IL) with a monoclonal mouse anti-V5 antibody (Abcam). The eluate samples from the immunoprecipitation reactions were subjected to SDS-PAGE. The resulting gels were dried, and levels of radioactively labelled protein were determined by autoradiography.

mRNA expression

Lymphoblastoid cell lines from which the 288 DNA samples used for gene resequencing had been obtained were purchased from the Coriell Institute. Total RNA was extracted, and mRNA expression analysis was performed using the Affymetrix Human Genome U133 Plus 2.0 Array as described previously (Moyer *et al.*, 2008). Data from IMPDH2 probe set 201892_s_at were used to perform association analyses. *IMPDH2* mRNA expression levels for 30 randomly selected samples were also determined using SYBR® Green-based quantitative reverse transcription polymerase chain reaction (qRT-PCR).

Electrophoretic mobility shift assays

Electrophoretic mobility shift (EMS) assays were performed as described previously (Moyer *et al.*, 2008). Sp1 antibody (Santa Cruz Biotechnology, Santa Cruz, CA), 400 μg·mL^{-1}, was used to perform supershift assays.

Structural analysis

The human IMPDH1 and IMPDH2 crystal structures were used to perform computational modelling of variant allozymes. For IMPDH1, a 2.5 Å resolution crystal structure bound to the substrate analogue 6-chloropurine riboside 5′-monophosphate (6-Cl-IMP) was used as a starting template (PDB ID: 1JCN; Risal *et al.*, unpublished). A 2.65 Å resolution structure of IMPDH2 bound to two inhibitors, C2-mycophenolic adenine dinucleotide and ribavirin monophosphate, was used for that enzyme (PDB ID: 1NF7; Risal *et al.*, unpublished). Molecular visualization and computational modelling of the variants was performed using Coot (Emsley and Cowtan, 2004). To computationally probe possible structural consequences in more detail, molecular dynamics simulations of both WT and variant allozymes were attempted using the GROMACS3.3.3 software package (Van Der Spoel *et al.*, 2005). Unfortunately, those simulations were unstable, presumably due to the incomplete nature of the starting crystal structures (95 missing residues in five gaps for IMPDH1 and 71 residues in four gaps for IMPDH2). Structural figures were prepared with Molscript and Raster3D (Kraulis, 1991; Merritt and Bacon, 1997).

Data analysis

Gene sequencing chromatograms were analysed with Mutation Surveyor (SoftGenetics, State College, PA). Linkage disequilibrium was determined by calculating r^2 and D' values (Hedrick, 2000; Hartl and Clark, 2007), and intragene haplotypes were inferred as described by Tajima (Schaid *et al.*, 2002). Values for π, θ and Tajima's D were calculated as described previously (Tajima, 1989a,b). Genotype–phenotype correlations for *IMPDH2* SNPs with $\log_2$-transformed *IMPDH2* mRNA expression

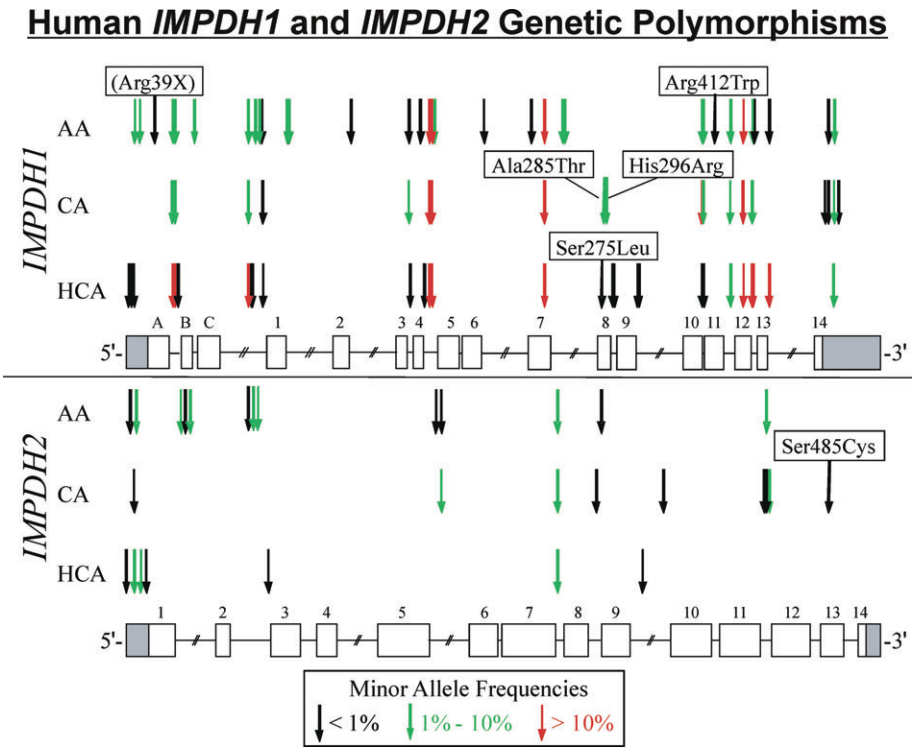

Figure 1

Human *IMPDH1* and *IMPDH2* genetic polymorphisms. Open rectangles denote coding exons, and shaded rectangles are untranslated regions. The exons for *IMPDH1* are numbered according to Gu *et al.* (1997), so that translation initiation for the canonical 514 amino acid IMPDH1 isoform begins in exon 1. Exons A, B and C encode N-terminal extensions that are part of longer IMPDH1 isoforms that are translated from an ATG translation initiation codon located in exon A. Arrows indicate the locations of polymorphisms, with frequencies indicated by colours. Nonsynonymous SNPs are indicated, with the appropriate amino acid change. AA, African-American; CA, Caucasian-American; HCA, Han Chinese-American.

levels were calculated separately for each ethnic group using PLINK (Purcell *et al.*, 2007). Transcription factor binding sites were predicted using TFSEARCH v.1.3 (Heinemeyer *et al.*, 1998). Apparent K_M values were calculated using Prism 4 (GraphPad Software, La Jolla, CA). Average levels of allozyme activity and protein were compared using the two-sample *t*-test assuming unequal variance (Microsoft Excel, Redmond, WA).

Results

Gene sequencing

We resequenced *IMPDH1* and *IMPDH2* using DNA from 288 healthy individuals divided equally among three ethnic groups. The cell lines used to isolate this DNA were deposited by the National Institute of General Medical Sciences, in part, to help create a resource for defining common genetic variation across ethnic groups for use in pharmacogenetic studies. Healthy subjects were used to avoid 'enrichment' for any particular disease. We observed 73 SNPs – 59 novel (previously unavailable in public databases) – for *IMPDH1*, including four nonsynonymous SNPs. For *IMPDH2*, 25 SNPs – 24 novel – were observed, including one nonsynonymous SNP (Figure 1 and Table 1). We have used the nomenclature of Gu *et al.* (1997) for *IMPDH1* and will refer to the differentially expressed 5′-exons as 'A', 'B' and 'C'. The exon A (115) SNP (Arg39X) results in a truncating mutation in longer IMPDH1 isoforms. Our gene resequencing data were deposited in the National Institutes of Health-supported pharmacogenetics database PharmGKB (Submission IDs: PS208272 for *IMPDH1*, and PS208273 for *IMPDH2*) and in dbSNP. All SNPs were in Hardy–Weinberg equilibrium ($P > 0.001$). Polymorphism locations and frequencies varied widely among the three ethnic groups. *IMPDH1* had 49, 26 and 39 SNPs in the AA, CA and HCA populations, respectively, but only 20 were found in more than one population. For *IMPDH2*, there were 11, 8 and 3 SNPs in the AA, CA and HCA populations, respectively, but only one of these SNPs was observed in all three populations.

The extent of genetic variation within resequenced areas was estimated by calculating π, an estimate of average heterozygosity per site, and θ, a

Table 1

Human *IMPDH1* and *IMPDH2* genetic polymorphisms

IMPDH isoform	Polymorphism location	HGVS nomenclature[a]	Nucleotide sequence change	Amino acid sequence change	Minor allele frequency			Previously reported	rs Number
					AA	CA	HCA		
1	5′-FR (−1262)	−1262	T > C		0.010	0.000	0.000		rs72624920
1	5′-FR (−1195)	−1195	C > A		0.000	0.000	0.005		rs72624921
1	5′-FR (−1061)	−1061	C > G		0.010	0.000	0.000		rs72624922
1	5′-FR (−1000)	−1000	del TAACA		0.010	0.000	0.031		rs72624923
1	5′-FR (−992)	−992	C > A		0.063	0.073	0.198		rs72624924
1	5′-FR (−980)	−980	ins TAAAA		0.010	0.000	0.031		rs72624925
1	5′-FR (−969)	−969	ins AAAAT		0.000	0.000	0.005		rs72624926
1	5′-FR (−791)	−791	C > G		0.000	0.000	0.026		rs72624927
1	5′-FR (−751)	−751	G > T		0.083	0.167	0.000		rs72624928
1	5′-FR (−743)	−743	T > C		0.063	0.026	0.182		rs72624929
1	5′-FR (−572)	−572	G > A		0.036	0.000	0.000		rs72624930
1	5′-FR (−493)	−493	C > T		0.005	0.021	0.000		rs72624931
1	5′-FR (−467)	−467	G > A		0.010	0.000	0.000		rs72624932
1	5′-FR (−462)	−462	T > C		0.016	0.130	0.026	Yes	rs11761662
1	5′-FR (−434)	−434	C > T		0.000	0.000	0.010		rs72624933
1	5′-UTR (−301)	−301	G > A		0.000	0.000	0.005		rs66539932
1	5′-UTR (−184)	−184	C > T		0.000	0.000	0.005		rs72624934
1	5′-UTR (−181)	−181	G > C		0.000	0.000	0.005		rs72624935
1	5′-UTR (−69)	−69	T > G		0.016	0.000	0.000		rs72624936
1	5′-UTR (−36)	−36	T > C		0.005	0.000	0.000		rs72624937
1	Exon A (115)	115	C > T	(Arg39X)[b]	0.005	0.000	0.000		rs72624938
1	IVS A (−52)	147−52	G > T		0.063	0.026	0.182	Yes	rs2288552
1	IVS A (−35)	147−35	G > A		0.063	0.026	0.182	Yes	rs2288551
1	IVS A (−26)	147−26	C > A		0.000	0.000	0.005		rs72624939
1	IVS B (49)	190+49	G > A		0.047	0.000	0.000		rs72624940
1	IVS C (−850)	255−850	A > C		0.011	0.052	0.297	Yes	rs28364722
1	IVS C (−823)	255−823	G > A		0.000	0.000	0.005		rs72624941
1	IVS C (−713)	255−713	G > A		0.000	0.000	0.005		rs72624942
1	IVS C (−531)	255−531	G > A		0.042	0.000	0.000		rs72624943
1	IVS C (−530)	255−530	A > C		0.021	0.000	0.000		rs72624944
1	IVS C (−94)	255−94	C > T		0.000	0.005	0.000		rs72624945
1	IVS C (−58)	255−58	G > C		0.005	0.000	0.000		rs72624946
1	IVS C (−36)	255−36	C > A		0.000	0.000	0.005		rs72624947
1	IVS 1 (7)	353+7	G > C		0.021	0.000	0.000		rs72624948
1	IVS 1 (46)	353+46	G > A		0.005	0.000	0.000		rs72624949
1	IVS 1 (120)	353+120	C > A		0.058	0.000	0.000		rs72624950
1	IVS 2 (57)	402+57	G > A		0.005	0.000	0.000		rs72624951
1	IVS 3 (−34)	505−34	C > A		0.005	0.021	0.000		rs72624952
1	IVS 3 (−10)	505−10	T > C		0.000	0.000	0.005		rs72624953
1	Exon 4 (306)	306	C > T		0.005	0.000	0.000	Yes	rs34724843
1	IVS 4 (16)	579+16	G > T		0.000	0.000	0.005		rs72624954
1	IVS 4 (119)	579+119	G > A		0.458	0.510	0.385	Yes	rs2278293
1	IVS 4 (−106)	580−106	G > A		0.427	0.370	0.521	Yes	rs2278294
1	IVS 4 (−69)	580−69	C > T		0.010	0.000	0.000		rs72624955

Table 1

Continued

IMPDH isoform	Polymorphism location	HGVS nomenclature[a]	Nucleotide sequence change	Amino acid sequence change	Minor allele frequency			Previously reported	rs Number
					AA	CA	HCA		
1	IVS 6 (58)	874+58	G > A		0.005	0.000	0.000		rs72624956
1	Exon 7 (633)	633	C > T		0.005	0.000	0.000		rs72624957
1	Exon 7 (732)	732	G > C		0.104	0.151	0.151	Yes	rs2288550
1	IVS 7 (6)	1074+6	G > T		0.010	0.000	0.000	Yes	rs61751224
1	IVS 7 (7)	1074+7	C > T		0.010	0.000	0.000		rs72624958
1	IVS 7 (102)	1074+102	C > T		0.010	0.000	0.000		rs72624959
1	Exon 8 (824)	824	C > T	Ser275Leu	0.000	0.000	0.005		rs72624960
1	Exon 8 (853)	853	G > A	Ala285Thr	0.000	0.010	0.000		rs72624961
1	Exon 8 (887)	887	A > G	His296Arg	0.000	0.010	0.000	Yes	rs61751223
1	IVS 8 (14)	1165+14	C > T		0.000	0.000	0.005		rs72624962
1	IVS 8 (–45)	1166–45	G > A		0.000	0.000	0.005		rs72624963
1	IVS 9 (12)	1261+12	G > A		0.000	0.000	0.005		rs72624964
1	IVS 9 (29)	1261+29	G > A		0.000	0.000	0.005		rs72624965
1	IVS 10 (9)	1405+9	A > G		0.000	0.000	0.011	Yes	rs11562030
1	IVS 10 (33)	1405+33	C > T		0.083	0.167	0.000	Yes	rs28580600
1	IVS 10 (53)	1405+53	del G		0.021	0.026	0.182		rs72624966
1	Exon 11 (1234)	1234	C > T	Arg412Trp	0.005	0.000	0.000		rs72624967
1	IVS 11 (176)	1550+176	T > G		0.010	0.052	0.260	Yes	rs4731447
1	Exon 12 (1320)	1320	G > A		0.266	0.255	0.349	Yes	rs2228075
1	IVS 12 (33)	1694+33	C > T		0.000	0.016	0.000		rs72624968
1	IVS 12 (43)	1694+43	G > A		0.010	0.052	0.260		rs72624969
1	IVS 12 (59)	1694+59	G > T		0.005	0.000	0.000		rs72624970
1	IVS 12 (–24)	1695–24	C > T		0.005	0.000	0.000		rs72624971
1	IVS 13 (27)	1778+27	A > C		0.005	0.000	0.000		rs72624972
1	3′-UTR (1682)	*1682	G > C		0.000	0.005	0.000		rs72624973
1	3′-UTR (1741)	*1741	C > T		0.005	0.005	0.000		rs72624974
1	3′-UTR (1772)	*1772	C > T		0.000	0.000	0.010		rs72624975
1	3′-UTR (1773)	*1773	G > A		0.010	0.042	0.000		rs72624976
1	3′-UTR (1821)	*1821	C > T		0.000	0.005	0.000		rs72624977
2	5′-FR (–619)	–619	G > T		0.000	0.000	0.005		rs72639215
2	5′-FR (–398)	–398	C > A		0.005	0.000	0.000		rs72639216
2	5′-FR (–274)	–274	C > T		0.000	0.005	0.000		rs72639217
2	5′-FR (–207)	–207	del TGG		0.000	0.000	0.016		rs72639218
2	5′-FR (–162)	–162	C > T		0.042	0.000	0.000		rs72639219
2	5′-FR (–118)	–118	C > T		0.000	0.000	0.016		rs72624903
2	5′-UTR (–69)	–69	C > T		0.000	0.000	0.005		rs72624904
2	IVS 1 (91)	98+91	T > G		0.010	0.000	0.000		rs72639213
2	IVS 1 (93)	98+93	G > C		0.005	0.000	0.000		rs72639214
2	IVS 1 (–4)	99–4	G > A		0.016	0.000	0.000		rs72624905
2	IVS 2 (21)	147+21	G > T		0.005	0.000	0.000		rs72624906
2	IVS 2 (65)	147+65	C > G		0.016	0.000	0.000		rs72624907
2	IVS 2 (–77)	148–77	C > T		0.016	0.000	0.000		rs72624908
2	IVS 2 (–64)	148–64	G > C		0.000	0.000	0.005		rs72624909
2	IVS 5 (–112)	532–112	A > G		0.005	0.000	0.000		rs72624910

Table 1

Continued

IMPDH isoform	Polymorphism location	HGVS nomenclature[a]	Nucleotide sequence change	Amino acid sequence change	Minor allele frequency AA	CA	HCA	Previously reported	rs Number
2	IVS 5 (–96)	532–96	G > A		0.005	0.031	0.000		rs72624911
2	IVS 7 (10)	819+10	T > C		0.031	0.083	0.031	Yes	rs11706052
2	IVS 8 (26)	910+26	A > G		0.000	0.005	0.000		rs72624912
2	Exon 9 (999)	999	G > A		0.005	0.000	0.000		rs72624913
2	IVS 9 (108)	1006+108	C > G		0.000	0.000	0.005		rs72624914
2	IVS 9 (202)	1006+202	C > T		0.000	0.005	0.000		rs72624915
2	IVS 11 (25)	1295+25	C > T		0.000	0.005	0.000		rs72624916
2	IVS 11 (44)	1295+44	C > T		0.010	0.005	0.000		rs72624917
2	IVS 11 (71)	1295+71	C > T		0.000	0.031	0.000		rs72624918
2	Exon 13 (1454)	1454	C > G	Ser485Cys	0.000	0.005	0.000		rs72624919

Polymorphisms in *IMPDH1* exons and untranslated regions (UTRs) are numbered relative to the A (nucleotide 1) in the ATG translation initiation codon located in exon 1 of the canonical 514 amino acid isoform. Negative numbers are assigned to positions 5′ to that location, and positive numbers for positions 3′ to the A in that ATG. Nucleotides located within introns (IVSs) are numbered based on their distance from the nearest splice junction, with distances from 3′-splice junctions assigned positive numbers, and distances from 5′ splice junctions assigned negative numbers. Exons A, B and C encode N-terminal extensions that are part of longer isoforms of IMPDH1, which are translated from an upstream ATG translation initiation codon located in exon A (see Figure 1). Amino acid changes due to nonsynonymous SNPs are numbered for the canonical 514 amino acid isoform of IMPDH1. Polymorphisms in *IMPDH2* are numbered in the same fashion relative to the A (nucleotide 1) in the ATG translation initiation codon. Polymorphisms identified previously are noted. Most of the rs numbers were assigned based on data from the present resequencing studies.

[a]The HGVS column reflects the Human Genome Variation Society nomenclature system described by Ogino *et al.* (2007).

[b]This SNP results in a truncating mutation for the longest, 599 amino acid isoform, of IMPDH1 at Arg39 (numbered from the upstream translation initiation codon).

SNP, single nucleotide polymorphism.

Table 2

π, θ and Tajima's *D* values for *IMPDH1* and *IMPDH2* in three ethnic groups

	Population	π ($\times 10^4$)	θ ($\times 10^4$)	Tajima's *D*	*P*-value
IMPDH1	AA	4.64 ± 2.66	11.1 ± 2.89	–1.72	0.081
	CA	4.75 ± 2.71	6.15 ± 1.78	–0.632	0.542
	HCA	6.78 ± 3.69	8.13 ± 2.23	–0.479	0.645
IMPDH2	AA	0.485 ± 0.54	3.20 ± 1.10	–2.11	0.030
	CA	0.485 ± 0.54	2.21 ± 0.86	–1.78	0.070
	HCA	0.236 ± 0.36	1.72 ± 0.74	–1.84	0.060

Values are normalized parameter estimates ± SE. The *P*-values listed refer to Tajima's *D*.

AA, African-American; CA, Caucasian-American; HCA, Han Chinese-American.

population mutation estimate of the neutral mutation variable. Tajima's *D*, a measure of the neutral mutation hypothesis that equals 0 under conditions of neutrality, was also calculated (Table 2) (Tajima, 1989a,b). *IMPDH2* values for π and θ were lower than those for *IMPDH1*. Tajima's *D* differed significantly from 0 only for *IMPDH2* in the AA population (Table 2). These results may be relevant to human evolution, but would not be expected to be directly related to drug response phenotypes.

IMPDH1 and *IMPDH2* haplotypes were inferred as described previously (Schaid *et al.*, 2002), and haplotypes with a frequency of ≥1% in any population, as well as those containing nonsynonymous SNPs, are listed in Tables S2 and S3 respectively. The haplotype nomenclature used in those tables assigns

a number to each haplotype containing a nonsynonymous SNP, corresponding to the order of appearance of nonsynonymous SNPs from 5′ to 3′, with letters corresponding to each haplotype in order of decreasing haplotype frequency.

Enzyme activity and substrate kinetics

IMPDH1 and IMPDH2 variant allozymes encoded by alleles with nonsynonymous SNPs were characterized functionally. To do that, WT IMPDH1 and IMPDH2, as well as the five variant allozymes observed during the resequencing studies, were transiently expressed in COS-1 cells to ensure the presence of mammalian post-translational modification and protein degradation systems. We also included the previously reported IMPDH2 Phe263 allozyme in these studies because of its reported reduced k_{cat} value (Wang *et al.*, 2007) and to provide as comprehensive functional genomic data as possible for these important genes. After correcting for transfection efficiency, IMPDH1 Leu275 and IMPDH2 Phe263 showed striking decreases in enzyme activity (10.2 ± 2.0% and 21.4 ± 8.7% of WT levels, respectively, $P < 0.0001$) (Figure 2A).

Because decreased activity for variant allozymes might be due to alterations in substrate kinetics, we also attempted to determine apparent K_M values for both IMP and NAD^+ for the two allozymes that displayed striking decreases in activity. K_M values for IMPDH1 Leu275 could not be determined accurately because it had extremely low activity. Apparent K_M values of WT IMPDH1 for IMP and NAD^+ were 9.84 ± 3.52 and 14.5 ± 8.9 μM respectively. Similar values for WT IMPDH2 and IMPDH2 Phe263 were 23.7 ± 5.8 and 10.2 ± 3.6 μM for IMP ($P < 0.05$ when compared with WT IMPDH2); and 24.9 ± 10.2 and 14.8 ± 8.1 μM for NAD^+.

Western blot analysis

Decreased enzyme activity might also be due to reduced protein quantity, as reported previously for many genetically polymorphic enzymes (Weinshilboum and Wang, 2004; Ji *et al.*, 2007; Moyer *et al.*, 2008). Therefore, we performed quantitative Western blot analysis of recombinant IMPDH allozymes in the same cytosol preparations used to assay enzyme activity. After correcting for transfection efficiency, IMPDH1 Leu275 and IMPDH2 Phe263 expressed significantly less immunoreactive protein than did their respective WT allozymes ($P < 0.0001$, Figure 2B). Leu275 had 37 ± 15% of WT IMPDH1 protein, while Phe263 showed the most dramatic decrease, with only 5.7 ± 1.3% of the WT IMPDH2 value. These quantitative Western blot results were significantly correlated with levels of enzyme activity ($r = 0.92$, $P = 0.0011$, Figure 2C), indicating that

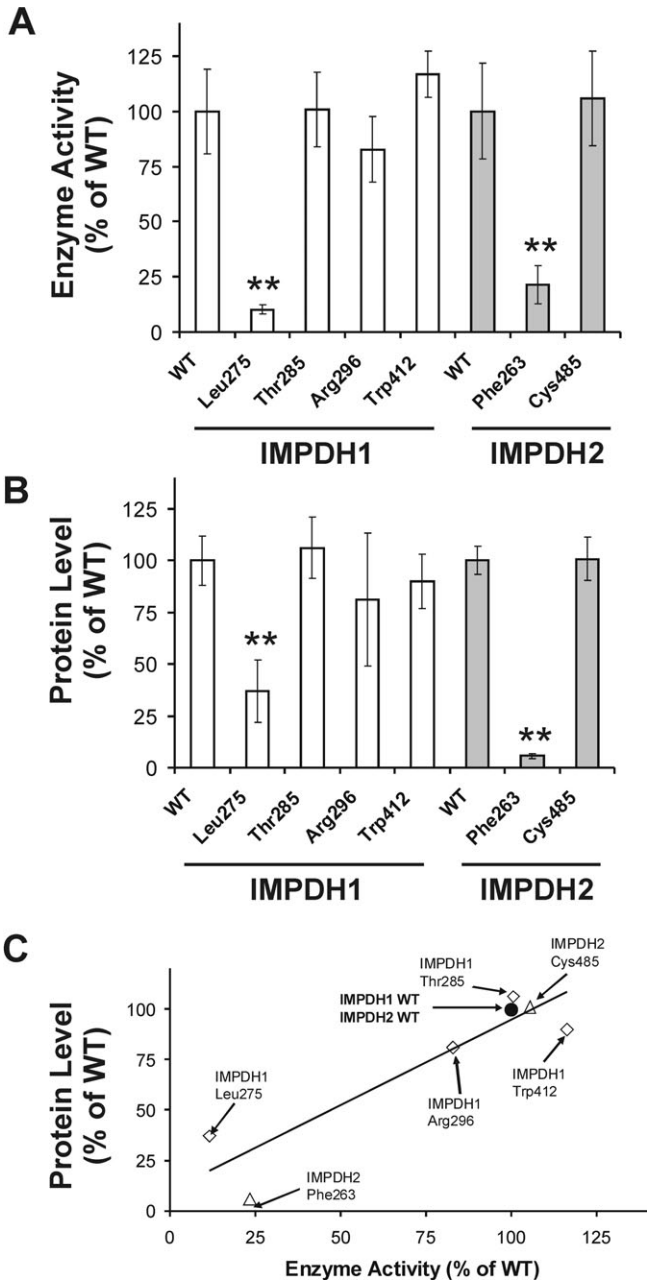

Figure 2

Average levels of *IMPDH1* and *IMPDH2* enzyme activity (A), and average levels of IMPDH1 and IMPDH2 immunoreactive protein levels (B), both expressed relative to values for the WT allozyme of the appropriate IMPDH isoform after the transfection of COS-1 cells. At least six independent experiments were performed for each allozyme, and results are expressed as a % of values for the WT allozyme. Error bars denote one SD. **Values that differ significantly from that of the appropriate WT allozyme at $P < 0.0001$. (C) Correlation between IMPDH1 and IMPDH2 allozyme enzyme activity and immunoreactive protein levels after expression in COS-1 cells ($r = 0.92$, $P = 0.0011$). The correlation coefficient for only IMPDH1 allozymes was $r = 0.93$ ($P = 0.021$), while that for only IMPDH2 allozymes was $r = 0.99$ ($P = 0.033$).

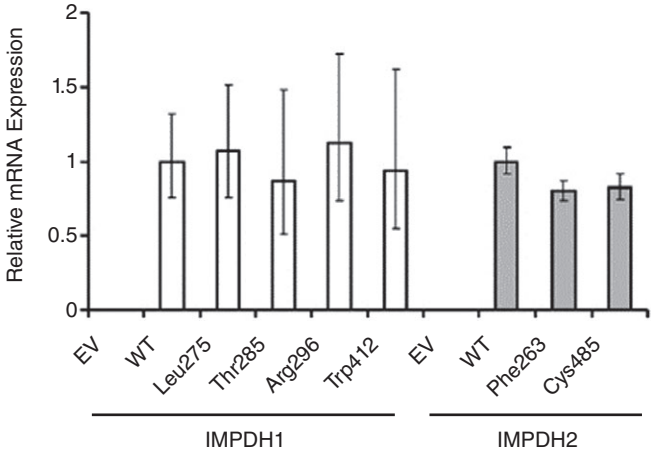

Figure 3

Average IMPDH1 and IMPDH2 allozyme mRNA expression levels as determined by qRT-PCR using SYBR Green chemistry. mRNA levels of IMPDH1 and IMPDH2 allozymes were measured relative to *lacZ* (which encodes β-galactosidase) mRNA levels, and were normalized to the appropriate WT mRNA level. Error bars denote 95% confidence intervals. EV denotes empty vector.

85% of the variation in level of enzyme activity might be explained by differences in quantity of immunoreactive protein (Figure 2C).

IMPDH mRNA levels

Decreased mRNA concentrations would be an additional possible explanation for decreased immunoreactive protein levels, perhaps as a result of decreased mRNA stability. Therefore, we performed qRT-PCR with total mRNA isolated from transiently transfected COS-1 cells, using co-transfected *lacZ*, which encodes β-galactosidase, to control for transfection efficiency. None of the IMPDH1 variant allozymes had an mRNA level that differed significantly from that for the WT allozyme (Figure 3), and while both IMPDH2 variant allozymes had slightly lower mRNA levels than did the WT, these small differences seemed unlikely to account for the observed differences in protein levels (Figure 2A).

In vitro *protein degradation*

Previous studies have shown that reduced protein levels for variant allozymes are often due to accelerated protein degradation (Wang *et al.*, 2003; Weinshilboum and Wang, 2004). Therefore, we performed *in vitro* degradation assays for IMPDH1 Leu275 and IMPDH2 Phe263 with an untreated RRL that contained all components of the ubiquitin proteasome degradation system. We were able to translate WT IMPDH1 and IMPDH2 as well as the two variant allozymes *in vitro* with similar efficiencies (Figure S1). However, only IMPDH1 Leu275 displayed accelerated degradation (Figure 4A and B).

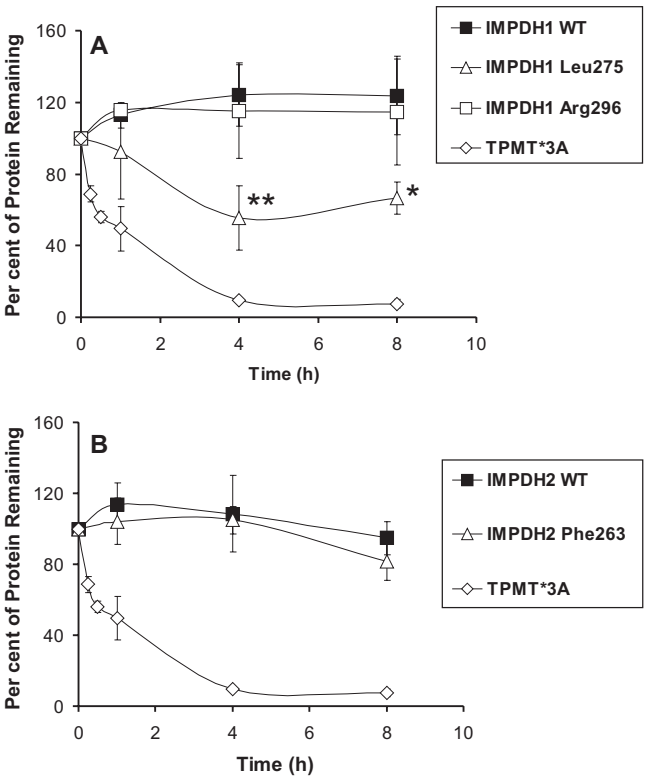

Figure 4

IMPDH1 and IMPDH2 rabbit reticulocyte lysate (RRL) degradation studies. Average levels of ^{35}S-labelled recombinant IMPDH1 (A) and IMPDH2 (B) allozyme protein remaining at 1, 4 and 8 h after incubation in an untreated RRL. Each time point represents the mean level of protein remaining relative to the initial protein level for three independent assays. Error bars denote one SD. *Differs from WT at this time point with $P < 0.05$. **Differs from WT at this time point with $P < 0.01$. The rapidly degraded TPMT*3A protein (Wang *et al.*, 2003) was included as a positive control.

TPMT*3A, a genetically variant allozyme that was previously shown to be rapidly degraded in the RRL (Wang *et al.*, 2003), was included in these assays as a positive control.

In vivo *pulse-chase assay*

Despite the low protein levels of IMPDH2 Phe263, we did not observe increased protein degradation for this variant *in vitro* using the RRL system. Because IMPDH2 Phe263 appeared to be transcribed and translated *in vitro* with efficiency similar to IMPDH2 WT, we performed an *in vivo* pulse-chase assay on COS-1 cells transiently expressing IMPDH2 WT or Phe263. A 27 h chase revealed that the Phe263 variant was being degraded at a significantly more rapid rate than the WT (Figure 5). These results, together with results from the *in vitro* degradation assay, suggest that levels of IMPDH2 Phe263 protein might be regulated, in part, by a protein

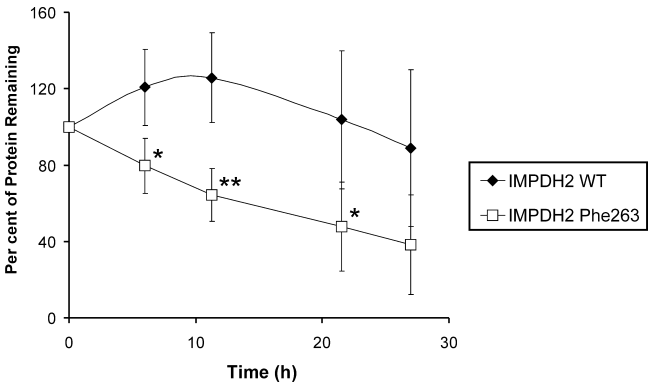

Figure 5

Pulse-chase assay for IMPDH2 WT and Phe263 allozymes. Recombinant IMPDH2 WT or Phe263 were transiently expressed in COS-1 cells, pulse-labelled with 0.1 mCi·mL^{-1} [^{35}S]-methionine, and chased with media containing excess non-radioactive methionine. Average level of ^{35}S-labelled protein remaining was determined at 6, 11, 21 and 27 h. Each time point represents the mean level of protein remaining relative to the initial protein level for four independent assays. Error bars denote one SD. *Differs from WT at this time point with $P < 0.05$. **Differs from WT at this time point with $P < 0.01$.

degradation system that requires intact cells – possibly via one of the autophagy pathways.

IMPDH variant allozyme structural analysis

Because of the striking decreases that we observed in cytosolic protein levels for IMPDH1 Leu275 and IMPDH2 Phe263 compared with WT (Figure 2B), and because those differences appeared to be due to accelerated degradation, perhaps as a result of protein misfolding (Wang *et al.*, 2005), we also used structural information to help interpret our observations. The Leu275 substitution in IMPDH1 was predicted to have a possible effect on enzyme structure and function. In the WT crystal structure, Ser275 was solvent-exposed and near the active site, with a closest approach of ~7 Å to the bound 6-Cl-IMP (Figure 6A). It was also near a subunit–subunit tetramer interface. Leu275 substitution might destabilize the WT conformation by introducing a large hydrophobic group at the surface, near the oligomerization interface. Increasing surface hydrophobicity could interfere with tetramerization and/or favour aggregation and membrane interaction, as the exposed hydrophobic residues would tend to interact with similar surfaces on other proteins. For Leu275 IMPDH1, substitution of the larger hydrophobic leucine for the smaller hydrophilic serine probably results in a local conformational change that might also alter enzyme activity as it is near the active site of the enzyme. In contrast, both Thr285 and Arg296 variants substitute hydrophilic residues at surface-exposed positions that are further from the active site and the tetramerization interface and therefore were not predicted to have significant effects on protein structure or function (Figure 6A). Trp412 altered a residue located in a gap in the crystal structure, so structural speculation was not possible.

The IMPDH2 Phe263 variant was also predicted to have unfavourable structural consequences. In the WT crystal structure, the Leu263 side chain was buried in a hydrophobic pocket and was distant from both the active site and tetramerization interface (Figure 6B). Computational substitution of the bulkier Phe263 residue would introduce a number of energetically unfavourable short contacts that could not be relieved with adjustment of only side chain conformation and would have a substantial effect on local protein conformation. Therefore, the Phe263 substitution would probably interfere with protein folding and/or stability. In contrast, the Cys485 IMPDH2 variant represented the conservative substitution of a hydrophilic solvent-exposed residue distant from both the active site and tetramerization interface. It could easily be accommodated by the WT protein conformation and, as a result, was thought to be unlikely to compromise folding and/or stability.

SNP-associated variation in mRNA levels

As intronic, 3′-FR or 5′-FR SNPs can influence transcription (Cheung *et al.*, 2005), we also attempted to determine whether SNPs outside of the open reading frames might be associated with *IMPDH1* and *IMPDH2* mRNA expression. We first obtained expression array data for the same lymphoblastoid cell lines from which the DNA used in our gene resequencing studies had been obtained. *IMPDH2* was highly expressed, but *IMPDH1* expression was too low to be measured reliably, so our analyses focused on *IMPDH2*.

Basal *IMPDH2* mRNA expression varied fivefold (Figure 7A), displayed a log-normal distribution (Figure 7B) and did not differ significantly across the three populations studied (Figure 7C). A random subset of the samples ($n = 30$) was used for qRT-PCR validation of the microarray results. The two sets of data were significantly correlated, with $r = 0.63$, $P = 0.0002$ (Figure S2). Subsequent SNP–expression association analyses showed that only a single *IMPDH2* SNP, IVS1(93), was significantly associated with basal mRNA expression ($P = 0.045$).

In order to determine whether IVS1(93) might be located within a sequence that could bind potential regulatory proteins, we performed EMS assays, assays that are used to investigate protein–DNA interactions. Our EMS assays showed that sequences containing IVS1(93) could bind nuclear extract

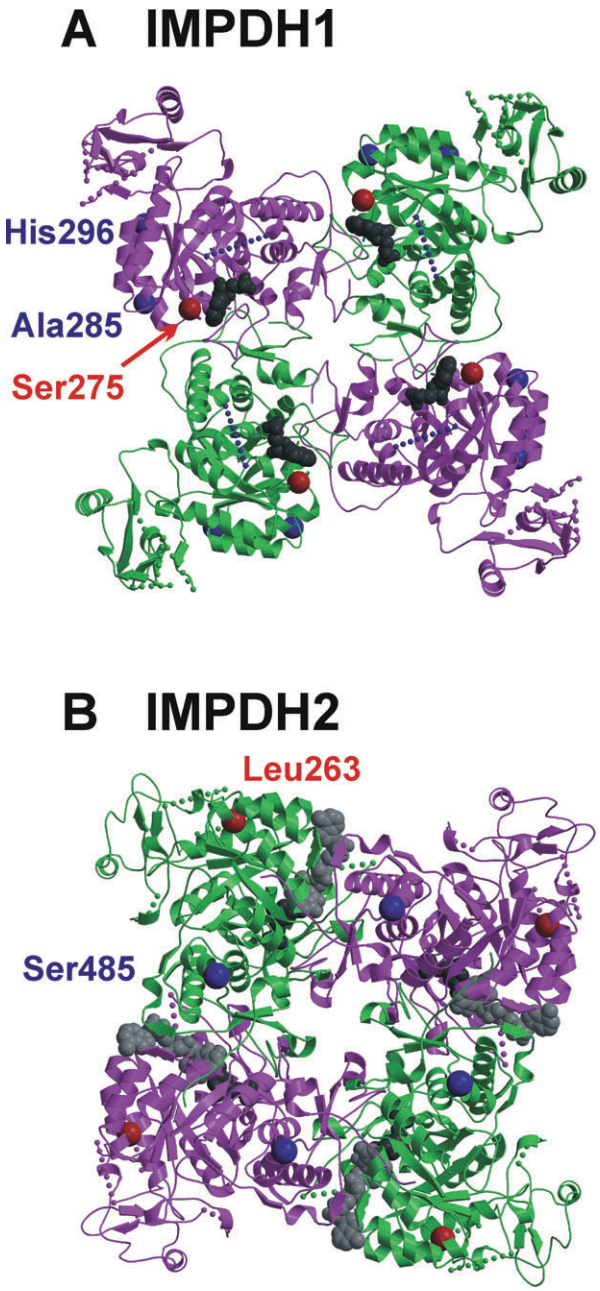

Figure 6

Variant residues within the IMPDH1 and IMPDH2 structures. (A) The tetrameric crystal structure of IMPDH1 is shown as a ribbon diagram (magenta and green) with five gaps for the missing residues within each monomer drawn as dotted lines. The active site bound inhibitor 6-Cl-IMP (shown as gray space-filling spheres) is accessible from the 'front' face. The WT amino acids at variant residues are depicted as red or blue spheres. Specifically, Ser275 (red sphere) is located near the active site and the tetramerization interface, while Ala285 and His296 (blue spheres) are distant from both. Arg412 is located in a gap of 50 disordered residues (blue dotted line), so its location cannot be shown. (B) The tetrameric IMPDH2 crystal structure containing ribavirin monophosphate (dark gray spheres) and C2-mycophenolic adenine dinucleotide (light gray spheres) in each active site is shown. From this 'back' view, both Leu263 (red sphere) and Ser485 (blue sphere) are distant from the active site and the tetramerization interface.

protein from these cells, resulting in a mobility shift of biotinylated DNA oligonucleotides from the region of unbound DNA oligonucleotides to 'Shift 1' and 'Shift 2' positions (Figure 7D, lane 2). The presence of the variant allele, however, abolished protein binding at 'Shift 2' (Figure 7D, lane 6). Because the WT sequence surrounding this SNP was predicted to bind to the transcription factor Sp1, while the variant nucleotide was predicted to abolish this putative binding site (Heinemeyer *et al.*, 1998), we attempted a 'supershift' assay with an Sp1 antibody. Addition of the antibody did not result in a 'supershift' above the original shifts, but the Sp1 antibody did attenuate protein binding (Figure 7D, compare lane 4 with lane 2).

Discussion and conclusions

We set out to identify and functionally characterize polymorphisms in *IMPDH1* and *IMPDH2*. Gene resequencing, performed with 288 DNA samples from three ethnic groups, resulted in the identification of 73 SNPs in *IMPDH1* (59 novel) and 25 SNPs in *IMPDH2* (24 novel). We then pursued the potential functional implications of nonsynonymous SNPs as well as SNPs that might alter transcription. Four nonsynonymous SNPs were identified in *IMPDH1* and one in *IMPDH2*, and we also performed functional genomic studies of the previously described IMPDH2 Phe263 allozyme (Wang *et al.*, 2007).

Two allozymes, IMPDH1 Leu275 (identified during our resequencing study) and IMPDH2 Phe263 (reported previously by Wang *et al.*, 2007), displayed striking decreases in cytosolic IMPDH activity (Figure 2). The decreased activity for IMPDH1 Leu275 could be explained, in part, by a decrease in immunoreactive protein (Figure 2B) caused by accelerated protein degradation (Figure 4A). This observation was supported by molecular modelling, which showed that the Leu275 substitution might compromise protein folding/tetramerization/stability and might also compromise enzyme activity by altering protein structure adjacent to the active site. The decreased activity of Phe263 correlated with a decrease in immunoreactive protein. Although neither changes in mRNA expression (Figure 3) nor *in vitro* protein degradation via ubiquitin-mediated proteasomal degradation could explain the decreased expression (Figure 4B), an *in vivo* pulse-chase assay showed that the decrease in immunoreactive protein for Phe263 could also be attributed to accelerated protein degradation (Figure 5), albeit through a process – possibly autophagy – that was not observed in the RRL system. These results also agreed with our structural

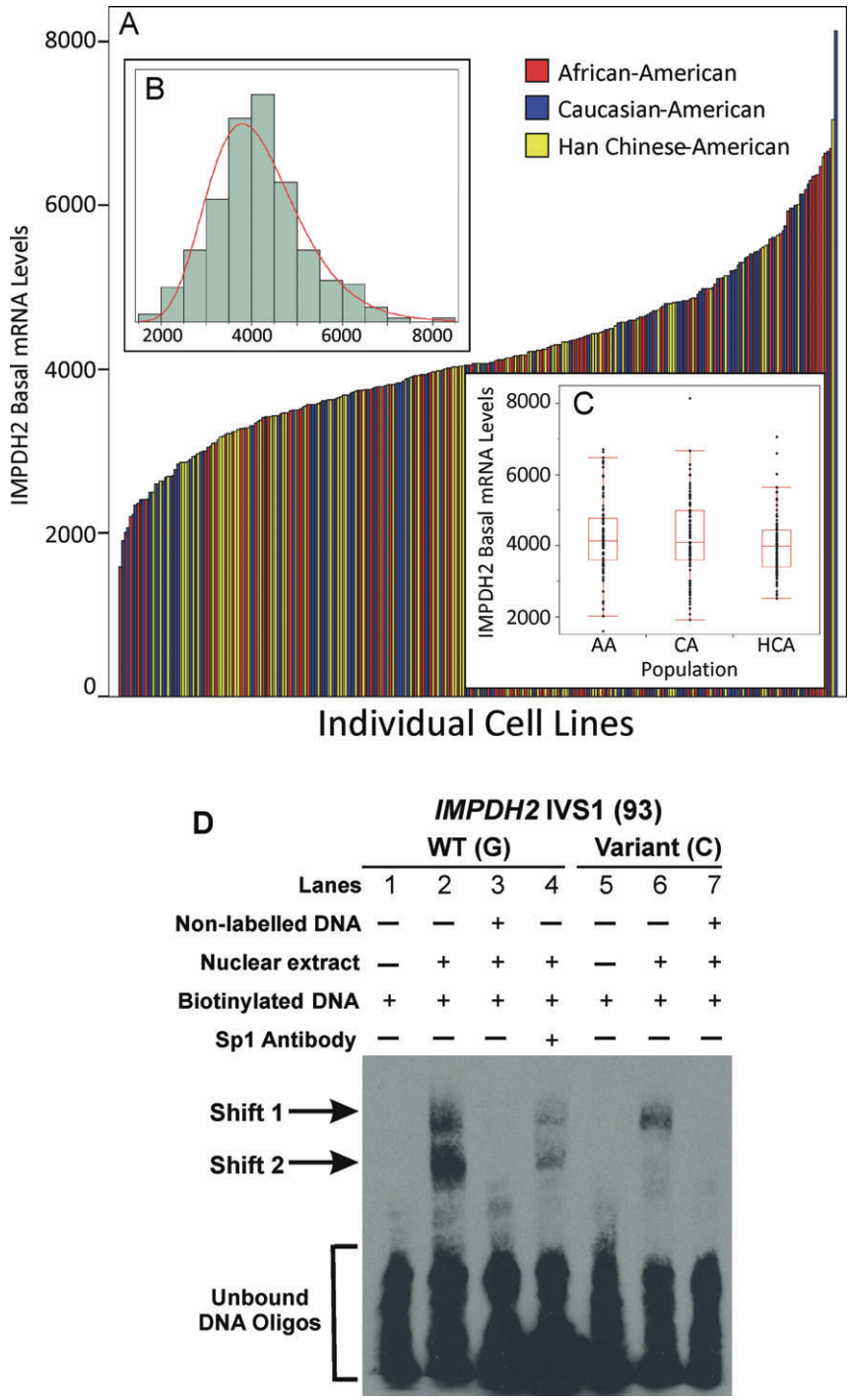

Figure 7

Basal *IMPDH2* mRNA expression levels in the lymphoblastoid cell lines from which the resequenced DNA was obtained. (A) Variation in *IMPDH2* basal mRNA expression levels. Each bar represents an individual cell line, and the height of the bar represents the basal mRNA expression level. Bars are colour-coded by ethnic group. (B) Frequency distribution histogram of *IMPDH2* basal mRNA expression levels. (C) *IMPDH2* basal mRNA expression did not differ across the three populations studied. AA, African-American; CA, Caucasian-American; HCA, Han Chinese-American. (D) Electrophoretic mobility shift assay blot for *IMPDH2* SNP IVS1(93) to investigate potential protein–DNA interactions. Lanes 1–4 contain DNA oligonucleotides with the WT sequence and lanes 5–7 contain DNA oligonucleotides with the variant nucleotide sequence. Lanes 1 and 5 contain no nuclear extract protein and serve as negative controls. Lane 2 shows that DNA oligonucleotides with the WT sequence result in two electrophoretic mobility shifts, 'Shift 1' and 'Shift 2'. Lane 6, which contains DNA oligonucleotides with the variant sequence, shows that the variant sequence cannot bind the protein(s) that result in 'Shift 2'. Lanes 3 and 7 contain excess non-labelled DNA oligonucleotides to show that the protein–DNA interactions seen in lanes 3 and 6 are specific. Addition of Sp1 antibody did not result in a supershift of either 'Shift 1' or 'Shift 2', but did attenuate both mobility shifts (lane 4).

modelling results, which showed that introduction of the bulky Phe263 residue was incompatible with the WT conformation and, as a result, could interfere with protein folding and/or stability. Our results extend the initial observation of low activity for Phe263 (Wang *et al.*, 2007) by suggesting that protein degradation may be a mechanism contributing to the decrease in activity. Although minor allele frequencies for these nonsynonymous SNPs are relatively low, Phe263, Leu275 and other, as yet unidentified rare variants of large effect in *IMPDH1* and *IMPDH2*, might have clinical significance.

In addition to alterations in function as a result of nonsynonymous SNPs, we also found that the *IMPDH2* IVS1(93) SNP was associated with a decrease in *IMPDH2* basal mRNA expression in lymphoblastoid cell lines. Furthermore, EMS assays showed that the variant nucleotide resulted in loss of nuclear extract protein binding (Figure 7D), perhaps by disrupting the binding of a transcription factor(s). These results will obviously require replication because of the low minor allele frequency of the IVS1(93) SNP.

Our results, in addition to providing insight into mechanisms by which *IMPDH1* and *IMPDH2* SNPs alter function, also provide polymorphism data that can be used to seek clinically relevant *IMPDH1* and *IMPDH2* SNP–expression or SNP–clinical phenotype correlations. The majority of the 73 SNPs that we observed in *IMPDH1* and the 25 SNPs we observed in *IMPDH2* were novel (previously unavailable in public databases). Because we utilized DNA from individuals representing three ethnic groups, we were also able to demonstrate that both genes display striking ethnic-dependent sequence variation, raising the possibility that patients from different ethnic groups might respond differently to 'standard' doses of MPA. For instance, the most common *IMPDH1* haplotype in AA and CA populations (**1A*), is relatively uncommon in the HCA population, and the second most common haplotype in the HCA population (**1R*, 18.7%) is not found in the AA population and is present at only a 3.1% frequency in the CA population (Table S2). As previous studies seeking to link genetic variation in *IMPDH1* and *IMPDH2* with response to MPA have primarily focused on Caucasians of European descent (Sombogaard *et al.*, 2009; Winnicki *et al.*, 2010) or on populations of undefined ethnicity (Wang *et al.*, 2007; 2008), our results will facilitate genotype–phenotype correlation studies performed with more diverse populations.

In summary, we have performed a comprehensive series of studies of common genetic variation in *IMPDH1* and *IMPDH2* in three populations and identified a novel nonsynonymous *IMPDH1* SNP associated with dramatically decreased activity. Our results have also provided insight into possible mechanisms by which SNPs in *IMPDH1* and *IMPDH2* could result in altered function. These observations will provide a foundation for future studies correlating sequence variation in these important genes with clinical outcome in patients being treated with MPA as well as future translational pharmacogenomic studies of MPA in transplantation recipients.

Acknowledgements

This work was supported in part by a Predoctoral Fellowship Award from the American Heart Association to T-Y Wu (09PRE2080377); by National Institutes of Health grants R01 GM28157, U01 GM61388 (The Pharmacogenetics Research Network) and R01 CA132780; and by a PhRMA Foundation 'Center of Excellence Award in Clinical Pharmacology'. We thank Judith Gilbert for advice with regard to the high performance liquid chromatography assays.

Conflict of interest

None.

References

Allison AC, Eugui EM (2000). Mycophenolate mofetil and its mechanisms of action. Immunopharmacology 47: 85–118.

Carr SF, Papp E, Wu JC, Natsumeda Y (1993). Characterization of human type I and type II IMP dehydrogenases. J Biol Chem 268: 27286–27290.

Cheung VG, Spielman RS, Ewens KG, Weber TM, Morley M, Burdick JT (2005). Mapping determinants of human gene expression by regional and genome-wide association. Nature 437: 1365–1369.

Emsley P, Cowtan K (2004). Coot: model-building tools for molecular graphics. Acta Crystallogr D Biol Crystallogr 60: 2126–2132.

Fernandez A, Martins J, Villlafruela JJ, Marcen R, Pascual J, Cano T *et al.* (2007). Variability of mycophenolate mofetil trough levels in stable kidney transplant patients. Transplant Proc 39: 2185–2186.

Glander P, Braun KP, Hambach P, Bauer S, Mai I, Roots I *et al.* (2001). Non-radioactive determination of inosine 5′-monophosphate dehydro-genase (IMPDH) in peripheral mononuclear cells. Clin Biochem 34: 543–549.

Glander P, Hambach P, Braun KP, Fritsche L, Giessing M, Mai I *et al*. (2004). Pre-transplant inosine monophosphate dehydrogenase activity is associated with clinical outcome after renal transplantation. Am J Transplant 4: 2045–2051.

Glander P, Sombogaard F, Budde K, van Gelder T, Hambach P, Liefeldt L *et al*. (2009). Improved assay for the nonradioactive determination of inosine 5′-monophosphate dehydrogenase activity in peripheral blood mononuclear cells. Ther Drug Monit 31: 351–359.

Gu JJ, Spychala J, Mitchell BS (1997). Regulation of the human inosine monophosphate dehydrogenase type I gene. Utilization of alternative promoters. J Biol Chem 272: 4458–4466.

Gu JJ, Stegmann S, Gathy K, Murray R, Laliberte J, Ayscue L *et al*. (2000). Inhibition of T lymphocyte activation in mice heterozygous for loss of the IMPDH II gene. J Clin Invest 106: 599–606.

Gu JJ, Tolin AK, Jain J, Huang H, Santiago L, Mitchell BS (2003). Targeted disruption of the inosine 5′-monophosphate dehydrogenase type I gene in mice. Mol Cell Biol 23: 6702–6712.

Hartl DL, Clark AG (2007). Principles of Population Genetics, 4th edn. Sinauer Associates: Sunderland, MA.

Hedrick PW (2000). Genetics of Populations, 2nd edn. Jones and Bartlett Publishers: Sudbury, MA.

Heinemeyer T, Wingender E, Reuter I, Hermjakob H, Kel AE, Kel OV *et al*. (1998). Databases on transcriptional regulation: TRANSFAC, TRRD and COMPEL. Nucleic Acids Res 26: 362–367.

Ji Y, Gu J, Makhov AM, Griffith JD, Mitchell BS (2006). Regulation of the interaction of inosine monophosphate dehydrogenase with mycophenolic acid by GTP. J Biol Chem 281: 206–212.

Ji Y, Moon I, Zlatkovic J, Salavaggione OE, Thomae BA, Eckloff BW *et al*. (2007). Human hydroxysteroid sulfotransferase SULT2B1 pharmacogenomics: gene sequence variation and functional genomics. J Pharmacol Exp Ther 322: 529–540.

Kraulis PJ (1991). MOLSCRIPT: a program to produce both detailed and schematic plots of protein structures. J Appl Crystallogr 19: 946–950.

Mak A, Cheak AA, Tan JY, Su HC, Ho RC, Lau CS (2009). Mycophenolate mofetil is as efficacious as, but safer than, cyclophosphamide in the treatment of proliferative lupus nephritis: a meta-analysis and meta-regression. Rheumatology (Oxford) 48: 944–952.

Merritt EA, Bacon DJ (1997). Raster3D: photorealistic molecular graphics. Methods Enzymol 277: 505–524.

Moyer AM, Salavaggione OE, Wu TY, Moon I, Eckloff BW, Hildebrandt MA *et al*. (2008). Glutathione S-transferase P1: gene sequence variation and functional genomic studies. Cancer Res 68: 4791–4801.

Ogino S, Gulley ML, den Dunnen JT, Wilson RB, Association E (2007). Standard mutation nomenclature in molecular diagnostics: practical and educational challenges. J Mol Diagn 9: 1–6.

Pisupati J, Jain A, Burckart G, Hamad I, Zuckerman S, Fung J *et al*. (2005). Intraindividual and interindividual variations in the pharmacokinetics of mycophenolic acid in liver transplant patients. J Clin Pharmacol 45: 34–41.

Purcell S, Neale B, Todd-Brown K, Thomas L, Ferreira MA, Bender D *et al*. (2007). PLINK: a tool set for whole-genome association and population-based linkage analyses. Am J Hum Genet 81: 559–575.

Schaid DJ, Rowland CM, Tines DE, Jacobson RM, Poland GA (2002). Score tests for association between traits and haplotypes when linkage phase is ambiguous. Am J Hum Genet 70: 425–434.

Senda M, Natsumeda Y (1994). Tissue-differential expression of two distinct genes for human IMP dehydrogenase (E.C.1.1.1.205). Life Sci 54: 1917–1926.

Sombogaard F, van Schaik RH, Mathot RA, Budde K, van der Werf M, Vulto AG *et al*. (2009). Interpatient variability in IMPDH activity in MMF-treated renal transplant patients is correlated with IMPDH type II 3757T > C polymorphism. Pharmacogenet Genomics 19: 626–634.

Spellicy CJ, Daiger SP, Sullivan LS, Zhu J, Liu Q, Pierce EA *et al*. (2007). Characterization of retinal inosine monophosphate dehydrogenase 1 in several mammalian species. Mol Vis 13: 1866–1872.

Tajima F (1989a). DNA polymorphism in a subdivided population: the expected number of segregating sites in the two-subpopulation model. Genetics 123: 229–240.

Tajima F (1989b). Statistical method for testing the neutral mutation hypothesis by DNA polymorphism. Genetics 123: 585–595.

Takebe N, Cheng X, Wu S, Bauer K, Goloubeva OG, Fenton RG *et al*. (2004). Phase I clinical trial of the inosine monophosphate dehydrogenase inhibitor mycophenolate mofetil (cellcept) in advanced multiple myeloma patients. Clin Cancer Res 10: 8301–8308.

Van Der Spoel D, Lindahl E, Hess B, Groenhof G, Mark AE, Berendsen HJ (2005). GROMACS: fast, flexible, and free. J Comput Chem 26: 1701–1718.

Wang L, Sullivan W, Toft D, Weinshilboum R (2003). Thiopurine S-methyltransferase pharmacogenetics: chaperone protein association and allozyme degradation. Pharmacogenetics 13: 555–564.

Wang L, Nguyen TV, McLaughlin RW, Sikkink LA, Ramirez-Alvarado M, Weinshilboum RM (2005). Human thiopurine S-methyltransferase pharmacogenetics: variant allozyme misfolding and aggresome formation. Proc Natl Acad Sci USA 102: 9394–9299.

Wang J, Zeevi A, Webber S, Girnita DM, Addonizio L, Selby R *et al*. (2007). A novel variant L263F in human inosine 5′-monophosphate dehydrogenase 2 is associated with diminished enzyme activity. Pharmacogenet Genomics 17: 283–290.

Wang J, Yang JW, Zeevi A, Webber SA, Girnita DM, Selby R *et al*. (2008). IMPDH1 gene polymorphisms and association with acute rejection in renal transplant patients. Clin Pharmacol Ther 83: 711–717.

Weinshilboum R, Wang L (2004). Pharmacogenetics: inherited variation in amino acid sequence and altered protein quantity. Clin Pharmacol Ther 75: 253–258.

Winnicki W, Weigel G, Sunder-Plassmann G, Bajari T, Winter B, Herkner H *et al*. (2010). An inosine 5′-monophosphate dehydrogenase 2 single-nucleotide polymorphism impairs the effect of mycophenolic acid. Pharmacogenomics J 10: 70–76.

Wu JC (1994). Mycophenolate mofetil: molecular mechanisms of action. Perspect Drug Discov 2: 185–204.

Zimmermann AG, Spychala J, Mitchell BS (1995). Characterization of the human inosine-5′-monophosphate dehydrogenase type II gene. J Biol Chem 270: 6808–6814.

Zimmermann AG, Wright KL, Ting JP, Mitchell BS (1997). Regulation of inosine-5′-monophosphate dehydrogenase type II gene expression in human T cells. Role for a novel 5′ palindromic octamer sequence. J Biol Chem 272: 22913–22923.

Supporting information

Additional Supporting Information may be found in the online version of this article:

Figure S1 Results of IMPDH1 and IMPDH2 allozyme *in vitro* translation using a rabbit reticulocyte lysate system.
Figure S2 qRT-PCR correlation with expression microarray results for *IMPDH2*.
Table S1 Sequences of primer pairs used to amplify *IMPDH1* and *IMPDH2* prior to resequencing
Table S2 *IMPDH1* haplotypes with frequencies of 1% or greater
Table S3 *IMPDH2* haplotypes with frequencies of 1% or greater

Please note: Wiley-Blackwell are not responsible for the content or functionality of any supporting materials supplied by the authors. Any queries (other than missing material) should be directed to the corresponding author for the article.